

Oxidative modification of skin lipids by cold atmospheric plasma (CAP): A standardizable approach using RP-LC/MS² and DI-ESI/MS²



Johanna Striesow^a, Jan-Wilm Lackmann^a, Zhixu Ni^{b,e}, Sebastian Wenske^a, Klaus-Dieter Weltmann^c, Maria Fedorova^{b,e}, Thomas von Woedtke^{c,d}, Kristian Wende^{a,*}

^a ZIK Plasmatis, Leibniz Institute for Plasma Science and Technology (INP Greifswald), Felix-Hausdorff-Straße 2, 17489 Greifswald, Germany

^b Center for Biotechnology and Biomedicine, University of Leipzig, Deutscher Platz 5, 04103 Leipzig, Germany

^c Leibniz Institute for Plasma Science and Technology (INP Greifswald), Felix-Hausdorff-Straße 2, 17489 Greifswald, Germany

^d Greifswald University Medicine, Fleischmannstraße 8, 17475 Greifswald, Germany

^e Institute of Bioanalytical Chemistry, Faculty of Chemistry and Mineralogy, University of Leipzig, Germany

ARTICLE INFO

Keywords:

Cold atmospheric plasma

Oxidative lipidomics

Lipid peroxidation

Skin lipids

Reactive oxygen and nitrogen species

ABSTRACT

Cold atmospheric plasma (CAP) is an emerging source for the locally defined delivery of reactive species, and its clinical potential has been identified in the control of inflammatory processes, such as acute and chronic wounds, or cancerous lesions. Lipids, due to their localization and chemical structure as ideal targets for oxidative species, are relevant modifiers of physiological processes. Human forehead lipids collected on a target were treated by an argon plasma jet and immediately analyzed by direct-infusion high-resolution tandem mass spectrometry (DI-MS²) or liquid chromatography-tandem MS (RP-LC/MS²). Subsequent data analysis was performed by LipidHunter (University of Leipzig), LipidXplorer (Max Planck Institute of Molecular Cell Biology and Genetics, Dresden), and LipidSearch (Thermo Scientific). With either MS method, all major lipid classes of sebum lipids were detected. Significant differences regarding triacylglycerols (predominantly identified in RP-LC/MS²) and ceramides (predominantly identified in DI-MS²) indicate experimental- or approach-inherent distinctions. A CAP-driven oxidation of triacylglycerols, ceramides, and cholesteryl esters was detected such as truncations and hydroperoxylations, but at a significantly lower extent than expected. Scavenging of reactive species due to naturally present antioxidants in the samples and the absence of a liquid interphase to allow reactive species deposition by the CAP will have contributed to the limited amount of oxidation products observed. In addition, limitations of the software's capability of identifying unexpected oxidized lipids potentially led to an underestimation of the CAP impact on skin lipids, indicating a need for further software development. With respect to the clinical application of CAP, the result indicates that intact skin with its sebum/epidermal lipid overlay is well protected and that moderate treatment will yield limited (if any) functional consequences in the dermal tissue.

1. Introduction

Cold atmospheric plasma (CAP) has emerged as a therapeutic alternative for conditions where redox-signaling processes are central—e.g., acute or chronic wounds (Emmert et al., 2013; Ulrich et al., 2015; Bekeschus et al., 2016; Weltmann and von Woedtke, 2017). Plasmas are gas-like systems and the fourth state of matter, following solid, liquid, and gaseous. All CAPs are composed of highly dynamic physical entities, such as electrons and higher energy states of atoms/molecules, ions, molecules, and radicals besides ultraviolet and visible radiation and electric fields. CAPs can be generated by various sources;

however, in the biomedical area, noble gas-driven plasma jets and dielectric barrier discharges are predominantly used (Emmert et al., 2013; von Woedtke et al., 2014; Bruggeman et al., 2016). The composition of the gaseous plasma phase is considerably well characterized—e.g., for the jet-based plasma sources kINPen (Reuter et al., 2012a; Schmidt-Bleker et al., 2014; Schmidt-Bleker et al., 2015a), RF jet (Zhang et al., 2013; Iseni et al., 2014; Van Ham et al., 2014), or COST-jet (Schneider et al., 2011; Golda et al., 2016; Gorbanov et al., 2018). In the case of the argon-based kINPen, major primary species in the gas phase are metastable argon (Ar^*) and argon excimers (Ar_2^*). Secondary gas phase species, formed by the interaction of primary

Abbreviations: CAP, cold atmospheric plasma; DI-MS², direct-infusion high-resolution tandem mass spectrometry; RP-LC/MS², reverse-phase liquid chromatography-tandem MS; Ar^* , metastable argon; Ar_2^* , argon excimers; NRF2, Nuclear factor erythroid 2-related factor 2; DDA, Data dependent analysis

* Corresponding author.

E-mail address: kristian.wende@inp-greifswald.de (K. Wende).

<https://doi.org/10.1016/j.chemphyslip.2019.104786>

Received 21 February 2019; Received in revised form 12 June 2019; Accepted 13 June 2019

Available online 20 June 2019

0009-3084/ © 2019 Published by Elsevier B.V.

species and feed gas admixtures (e.g., O₂ and N₂) or ambient species, include hydroxyl radicals (·OH), atomic oxygen (·O), singlet oxygen (¹O₂), ozone (O₃), atomic nitrogen (·N), and nitric oxides (N_xO_y) (Schmidt-Bleker et al., 2015b). If in contact with liquids, species such as hydrogen peroxide (H₂O₂), nitrite (NO₂⁻) or nitrate (NO₃⁻), peroxy nitrite (ONO⁻), or peroxy nitrate (OONOO⁻) are present or suspected (Winter et al., 2013; Lukes et al., 2014; Nakashima et al., 2016). By electron paramagnetic resonance spectroscopy, hydroxyl radicals (·OH), superoxide radicals (·O₂⁻), or nitric oxide (·NO) were detected (Tresp et al., 2013; Gorbanev et al., 2016; Jablonowski et al., 2018). By the interaction of primary or secondary species with ions or molecules of the treated target, additional species such as hypochlorite (OCl⁻) can evolve (Wende et al., 2015). These secondary species in liquids or liquid-like systems are of interest in biomedical research regarding the physiologic consequences they trigger. Current results show plasma-derived reactive species to modulate cellular redox signaling—e.g., activation of nuclear factor (erythroid-derived 2)-like 2 (NRF2)-dependent protein synthesis (Schmidt et al., 2015), p53-related regulation (Schmidt et al., 2019), or immunomodulatory effects (Bekeschus et al., 2018; Rödder et al., 2019). However, thus far, the exact biochemical pathways remain unclear. While long-lived reactive species have been reported to enter the cell via aquaporins (Yan et al., 2017), other results have indicated that the covalent modification of biomolecules contribute significantly. This has been extensively studied for amino acids (Takai et al., 2014; Zhou et al., 2016; Klinkhammer et al., 2017; Lackmann et al., 2018) and proteins (Lackmann et al., 2015; Choi et al., 2017).

Surprisingly, little is known about the potential of CAP-derived species for lipid oxidation. Due to the exposed location in the cell membrane and other biological barriers such as the skin, the presence of easily oxidized double bonds with its adjacent allylic positions must assume that CAP affects the structure and integrity of (polar) lipids and, consequently, cell membranes. A few papers have describe the oxidation of model lipids—e.g., DOPC and DMPC liposomes—by CAP. As expected, one of the targeted structures is the cis-Δ⁹ double bond of oleic acid, yielding (9-oxo-nonenoyl)-sn-glycero-3-phosphocholine (PoxnoPC) or chlorohydrins (Maheux et al., 2016; Yusupov et al., 2017). It was reported that CAP treatment of intact human skin mitigates the transport of large molecules through the *stratum corneum* (Lademann et al., 2011a, b). The mechanism has not been investigated in detail, but lipid oxidation might have contributed.

To test to what extent complex skin lipids are chemically modified by a plasma treatment, lipids were collected from human foreheads on glass slides and immediately treated by CAP. High-resolution mass spectrometry analysis of the lipids was achieved either by extracting the lipids directly from the surface combined with following direct infusion into the mass spectrometer using a robotic system (Advion NanoMate, static nanoelectrospray approach) or by a classic sample preparation and UHPLC separation before MS. The raw data obtained by both approaches were analyzed using three different software packages (LipidHunter/LPPTiger beta by the University of Leipzig, LipidXplorer by Max-Planck Institute Dresden, and Lipid Search by Thermo

Scientific) to ensure the highest identification rates and compare the respective bioinformatics work flow, especially regarding the identification of oxidized lipids.

2. Materials and methods

2.1. Collection of skin lipid samples

Lipids originating from the *stratum corneum* and sebum were collected from 22 healthy volunteers. The participants were of different ages (20–59 years) and genders (10 male and 12 female). All sampling from the participants was performed with informed consent. The sampling of forehead skin lipids was carried out on glass slides. The forehead area was cleaned with a sodium laureth sulfate-based neutral soap 15 min prior to sampling. A glass coverslip (18 × 18 mm) was placed on the forehead region and was lightly pressed for 15 s. For each participant, four glass slides of different but comparable forehead regions were sampled.

2.2. Plasma source and treatment

Of the four glass slides, two were used for treatment with a cold atmospheric plasma jet kINPen (neoplas tools GmbH, Germany, Fig. 1). The device consists of a grounded ring electrode and a ceramic capillary, where a centered rod electrode is located inside. A voltage of 2–6 kV_{pp} was applied to the central electrode with a frequency of 1.1 MHz. Argon (purity 99.999%) was used as the working gas with a flow rate of three standard liters per minute (Reuter et al., 2012b). The glass slides were placed under the effluent of the plasma jet with a distance of 9 mm, while spiral movements ensured homogeneous treatment. The treatment time was 30 s. This specific treatment time was already applied in several previous studies and investigated regarding reactive species deposition in liquids (Wende et al., 2014; Winter et al., 2014; Ulrich et al., 2015). Additionally, a pretest was performed with different treatment times and showed that 30 s is best suitable for the application, especially regarding the loss of lipids from the glass slide due to the gas flow of the plasma jet. Furthermore, it relates to the current clinical use in wound care (10–20 s cm⁻²).

2.3. Lipid extraction and sample preparation

Ammonium formate and ammonium acetate (MS-grade) were obtained from Sigma or Roth, respectively. Sodium sulfate was purchased from VWR. Methyl-tert-butyl ether (MTBE) and chloroform were purchased from Sigma. Formic acid was obtained from Fluka. Water, methanol, and isopropanol (all from ChemSolute, MS grade) were purchased from Th. Geyer. For direct infusion analysis (DI), lipids were extracted from the glass slides using a chloroform/methanol/isopropanol extraction solution (1:2:4, v/v) with 5 mM ammonium acetate as an additive. The extract was diluted 1:10 with extraction solution and was placed in an Eppendorf twin-tec 96-well plate. The extract was then transferred into the MS by a TriVersa NanoMate. The aspirated

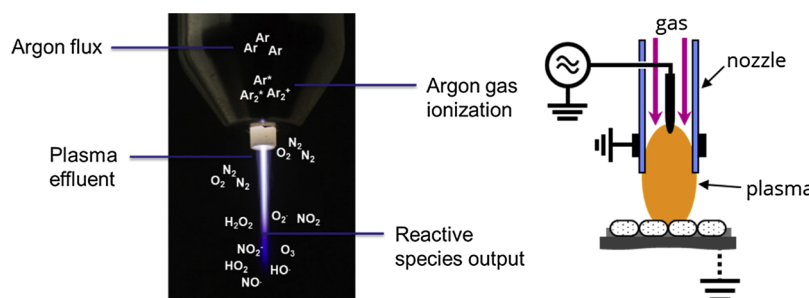


Fig. 1. Cold physical plasma device kINPen (argon-based plasma jet) photo and schematic treatment of a target (cells) (Weltmann et al., 2009).

volume of the extract was set to 5 μL , the gas pressure for the positive and negative ion mode was 0.40 psi, and the applied voltage was 1.50 kV. For RP-LC/MS² analysis, skin lipids were extracted using 70 μL of MTBE. Residual water was removed by sodium sulfate. The dehydrated extract was then placed in a preweighed vial (weighing error of analytical balance = 0.001 mg) to determine the amount of lipid sampled from each participant. The skin lipid extract was dried with argon gas and weighed again. Prior to liquid chromatography, the dried extract was suspended in methanol.

2.4. Direct-infusion MS²

For DI-MS² acquisition, a QExactive Plus mass spectrometer (Thermo Fisher) equipped with a TriVersa Nanomate ion source (Advion Biosciences) was used. The TriVersa Nanomate was operated in the static nanoelectrospray mode with a spray voltage of 3.50 kV and adjusted spray parameters for each polarity for stable spray conditions. Prior to injection, the lipid extract was mixed automatically by the device mandrel by mixing the solution several times to prevent a clogged injection needle. MS acquisition was carried out in both polarities with a resolving power of $\text{Rm/z}_{200} = 280.000$ in FullMS and $\text{Rm/z}_{200} = 70.000$ in MS². All MS² spectra were acquired in data-independent acquisitions (DIA) with an inclusion list adapted from a protocol by Eggers and Schwudke (2018). Briefly, an MS² spectrum was acquired every $m/z = 1.001$, starting from $m/z = 350.2$ in the positive polarity mode and $m/z = 350.1$ in the negative polarity mode. The collision energy (NCE) for MS² fragmentation was set to 30, and the method duration for each polarity was 5 min.

2.5. RP-LC/MS acquisition

For RP-LC/MS, a Vanquish UHPLC System equipped with an AccuCore C18+ column (2.1 \times 100 mm, 1.5 μm ; Thermo Fisher Scientific) was used. The injection volume was 1 μL . Every sample was measured in duplicate and in both polarities. The temperature of the column oven was set to 50 °C, and the used eluent system was methanol:water (A, v/v) at 50:50 and 100% isopropanol + 10 mM ammonium formate (B), both supplemented with 0.1% formic acid. The flow rate was 150 $\mu\text{L}/\text{min}$, starting from 5% B (Table 1).

MS acquisition was performed in the data-dependent acquisition (DDA) mode using the QExactive Plus mass spectrometer with a resolving power of $\text{Rm/z}_{200} = 70.000$ in the full MS mode and $\text{Rm/z}_{200} = 17.500$ in MS² and a scan range from m/z 150 to 2000. The normalized collision energy for MS² fragmentation was set to 25. The spray voltage on a HESI II ion source was set to 2.80 kV with adjusted spray parameters for stable spray conditions in each polarity. The run time was set to 60 min.

2.6. Lipid identification and data analysis

The direct infusion setup data were analyzed using LipidXplorer Software (Herzog et al., 2013). Mfql-files for lipid identification were adapted from LipidXplorer wiki and were adjusted to identify lipid oxidation (adjusted files, see supporting information). For

identification, only lipids with measured mass deviations below 2 ppm from MS and MS² peaks in scans were considered as positive hits and were used for data evaluation. The data from RP-LC/MS² measurements were analyzed using LipidSearch (Version 4.1.16; Thermo Fisher Scientific), and triacylglycerol analysis was performed using LipidHunter (Ni et al., 2017a, 2017b). For LipidSearch, the lipid identification workflow was set to a maximum precursor tolerance of 5 ppm, a maximum product tolerance of 7 ppm and an m-score threshold of 2.0. The top-ranked filter was enabled, and the main node filter was set to the main isomer peak. Fatty acid priority was enabled. The ID quality filter was set to A-B, allowing only identifications based on the overall structure, including the head group, glycerol backbone and fatty acid chains. All lipid classes were selected for identification. Ion adducts for positive mode measurements were $+H$, $+NH_4$, $+2H$ and those for negative mode measurements were $-H$, $+HCOO^-$ and $-2H$. After identification, the lipid species were filtered for peak quality (over 0.8) and the mass deviations were measured (between -1 and 1 ppm). Identification of oxidized lipid species with LipidSearch was performed with the inbuild OxGPL database, covering oxidative modifications of phospholipids, triacylglycerols, diacylglycerols and fatty acids. Oxidative modifications that this software is capable of detecting are additions of oxygen and the detection of truncations of fatty acid chains with additions of aldehyde-, carboxyl- and methylacetate groups. The analysis and identification of triacylglycerols were performed by Z. Ni (University of Leipzig) using the beta version of LipidHunter/LPPTiger for triacylglycerol and possible oxidative species identification. The provided data tables consisted of different DDA identifications (DDA 1–5), which were filtered for rank score (higher than 60) and a maximum mass deviation between -1 and 1 ppm. All the filtered DDA tables were summarized and presented as a heat map.

3. Results

3.1. Comparability of the lipid content before and after plasma treatment

The amount of sampled lipids subjected to MS did not change significantly by CAP treatment or gas flow (Fig. 2). The average sampled weight for lipids on the untreated glass slides was 0.39 mg/cm² ($SD = 0.11$) and 0.37 mg/cm² ($SD = 0.14$) for the lipids on the treated glass slides. This result showed that the total amount of lipids is not influenced by CAP treatment, and the data can be compared between the control and plasma-treated samples.

3.2. Identification of lipid classes and lipid oxidation by direct-infusion mass spectrometry

Raw data from DI-MS² analyzed with LipidXplorer show that all ten major lipid classes of the skin can be identified with different relative abundances (Fig. 3). All of these lipid classes were reportedly of epidermal origin or from the sebum. In all participants, high abundances of

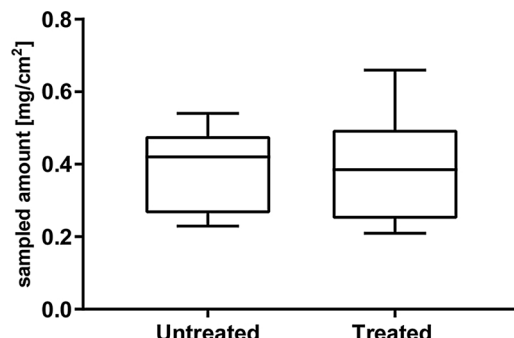


Fig. 2. Amount of skin-derived lipids sampled from participant's forehead on a glass slide (3.2 cm², $n = 22$) did not change significantly with treatment.

Table 1
Flow gradient for LC separation of skin lipids.

B [%]	Time [min]
5 % B	0 min
5 % B	5 min
90 % B	35 min
99 % B	36 min
99 % B	51 min
5 % B	52 min
5 % B	60 min

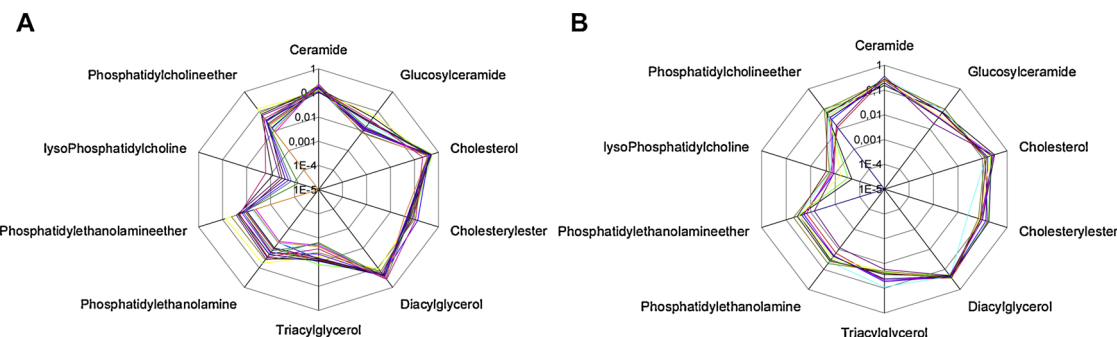


Fig. 3. Lipid classes identified by direct-infusion mass spectrometry and LipidXplorer in control (A) and CAP-treated (B) samples. The sum of all lipid species members (Native, oxidized) is shown. Only samples with sufficient data points in each lipid class are shown (untreated: n = 17; CAP-treated: n = 11).

ceramides, triglycerides, diglycerides, cholestryl esters, cholesterol, and phosphatidylcholine ethers were identified both in control and in treated samples. Lyso-phosphatidylethanolamine was only identified in treated samples (to facilitate comparison not shown in Fig. 3). In the group of triacylglycerols, a higher relative content of these lipids after treatment was observed. It was assumed, that this is the result of a diversification due to changes in the oxidative status of some triglycerides, increasing the sum of native, single- and double-oxidized lipid species. Additionally, oxidation leads to an increase of the molecules overall polarity, allowing a more effective dissolution during the direct-infusion approach and thereby increasing the molar fraction.

As assumed, the plasma-treated samples showed a triacylglycerol profile with a slightly higher amount of single oxidations (keto or hydroxyl group) and a decreasing abundance of native triacylglycerols. Additionally, changes in the classes of ceramides (increasing abundance of single-oxidized species) and cholestryl ester (decrease in native species) were visible. No differences were found in the abundance of native and oxidized species after treatment in the classes of glucosylceramides, cholesterol, phosphatidylethanolamines, and phosphatidylethanolamine ethers (Fig. 4).

To elucidate which lipid subspecies exactly showed a different oxidation pattern after plasma treatment, data analysis on the subspecies level was performed by calculating the ratios between the plasma-treated and untreated lipid species of the single-oxidized species of triacylglycerols, ceramides and cholestryl esters (Fig. 5).

A moderate increase in mono-oxidation after CAP treatment was

observed. Major targets were identified as cholestryl esters, triacylglycerols, and some ceramides. A significant interindividual variance can be observed while the presence of double bonds is not mandatory for oxidation events, e.g., in ceramides (Fig. 5B). The observed mono-oxidation of unsaturated molecules are related to the attack of atomic oxygen, yielding epoxides or ketones, while in saturated lipids hydroxylation following the attack of hydroxyl radicals were relevant.

3.3. Identification of lipid classes and lipid oxidation by LC/MS²

Compared with direct-infusion mass spectrometry, reversed-phase chromatographic separation in combination with HRMS was performed. Data analysis was performed with LipidSearch and LipidHunter/LPPTiger. LipidSearch identified nine major skin lipid classes in control and after CAP treatment, one class less than that identified by DI-MS². Cholesterol, glucosylceramides, phosphatidylethanolamines, phosphatidylethanolamine ethers and phosphatidylcholine ethers could not be identified using this approach. By contrast, monoacylglycerol and lyso-phosphatidylglycerols were found only with RP-LC/MS²/LipidSearch. Similar to DI-MS² measurements, the relative amount of triacylglycerol subspecies was higher after CAP treatment, indicating that better ionization or solubility is achieved by treatment (Fig. 6).

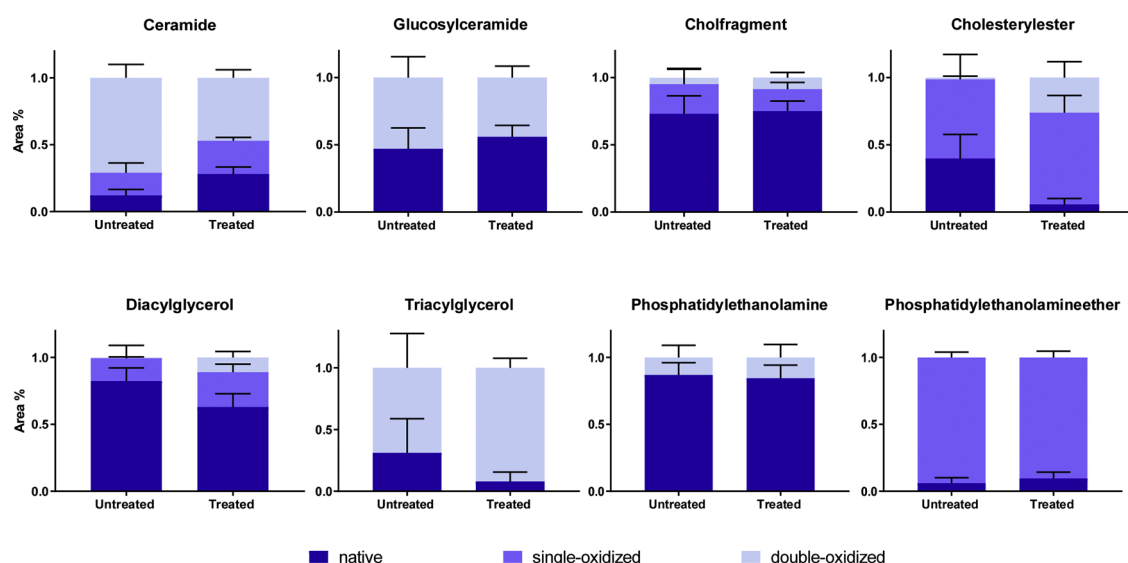


Fig. 4. Relative responses of the native and oxidized species of untreated and plasma-treated lipid classes. The responses of the native and oxidized species were normalized to the sum of the whole lipid class. Only participants with sufficient measured values were included (untreated: n = 17; CAP-treated: n = 11).

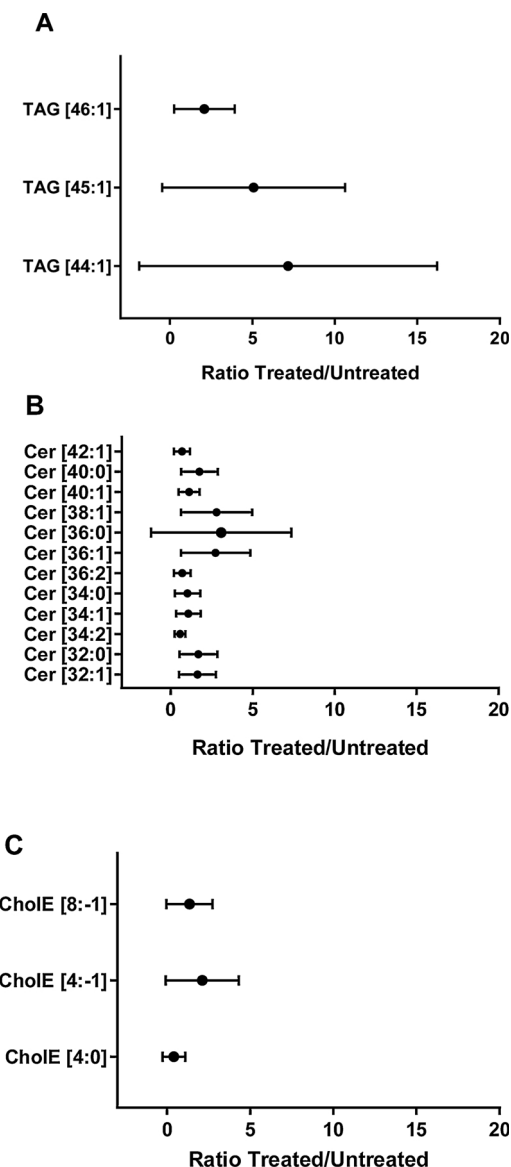


Fig. 5. Lipid species oxidation after CAP treatment (shown as the ratio between CAP-treated and untreated), mono-oxidized species ($Ox_1, m/z + 15.996$), triacylglycerols (TAG, A), ceramides (Cer, B), and cholesteryl esters (CholE, C), as measured by direct infusion HRMS and LipidXplorer data analysis.

3.4. Analysis of triacylglycerols using LipidHunter and LipidSearch

For further analysis of triacylglycerol subspecies and their oxidation by CAP, LipidSearch and LipidHunter/LPPTiger (Ni et al., 2017a, 2017b) software were compared. LipidSearch identified 141 triacylglycerol subspecies in the untreated and 111 triacylglycerol subspecies in the treated samples. LipidHunter identified 113 triacylglycerol subspecies in the untreated and 85 in the treated samples (Fig. 7). Interestingly, LPPTiger identified six oxidized triacylglycerol subspecies in the untreated samples, but no oxidation could be identified after CAP. The Venn diagram shows that 73 TGs are in common between the untreated and treated samples identified with LipidHunter and LipidSearch and that some subspecies are unique to the software used. LipidSearch identified a higher number of subspecies (41 more than LPPTiger for Triglycerols beta) but a strong overlap of 107 species was seen for both programs.

For a detailed analysis and an overview of all triacylglycerol subspecies identified using different software and in untreated and treated samples, the data were summarized in a heat map for each condition

and software used (Fig. 8 and Fig. S1 in supporting information). These data showed that the abundances of different triacylglycerol species vary from participant to participant underlining the expected intra-individual variability, but the range from TG 44:0 and 50:2 is well populated with some TGs commonly identified, e.g., TG 48:0. Highly abundant TGs contained completely saturated or one mono-unsaturated fatty acid residue. Two or three double bonds were found for a few TGs (e.g., 46:2, 50:2, 48:3), higher degrees of unsaturation were occasionally found in some individuals, e.g., for TG 54 (up to 54:7). After treatment, TGs containing double bonds decreased while the abundance variance increased (46:2, 46:3, 48:2, 48:3).

3.5. Identification of oxidized species after plasma treatment

Using the LPPTiger for triglycerides, no oxidation was detected in this lipid class, indicating an overall low abundance of oxidative changes. In a second approach to identify oxidized species, LipidSearch software was used in conjunction with the inbuild oxGPL database. Predominantly, a truncation of one fatty acid chain to a residual length between four and nine carbon atoms was observed. The terminal group was either an aldehyde or a carboxy group, in part esterified (methylated). For the TG 46:2 (18:2/14:0/16:0), the addition of three oxygen atoms was found, suggesting one allylic hydroperoxide and one hydroxyl group (presumably a decayed hydroperoxide) in the same molecule. The ratios of the measured peak areas between the identified oxidized species of CAP-treated and untreated samples showed three lipid oxidation products that were significantly increased in abundance after plasma treatment (Fig. 9). Surprisingly, these were the only oxidation products found by UHPLC/MS after CAP treatment. However, using the direct infusion approach, the number of oxidized species (+ one oxygen, LipidXplorer) was slightly higher (see Fig. 5). This suggests that the plasma treatment of skin lipids under normal (clinically applied) treatment conditions does not introduce a broad range of oxidation products.

4. Discussion

The aim of the present study was to investigate the impact of cold physical plasma (CAP) on a complex mixture of human lipids and matrix using a standardized approach. For ease of handling and safety precautions, an *ex vivo* model of the upper lipid layer of the forehead skin region were sampled. The cleaning process of the sampling area, the sampling, and lipid extraction were performed in a standardized manner according to a protocol applied to each participant to maximize comparability. This region is sebum rich. Cleaning the sampling region prior to collection of the samples and subsequent casual sebum production ensured a reproducible lipid film formation. Because only 15 min of sebum accumulation was allowed, a significant contribution of extracellular epidermal lipids was ensured. Sebum comprises triglycerides, free fatty acids, wax esters, squalene, and smaller amounts of cholesterol, cholesteryl esters, and diglycerides (Pappas, 2009; Akaza et al., 2014; Camera et al., 2016). Lipids of epidermal origin are a mixture of ceramides, free fatty acids and cholesterol. Lipids with a high degree of saturation can be found, except for the mono-unsaturated oleic (C18:1n-9) and sapienic acid (C16:1n-10). Additionally, natural antioxidants such as tocopherols, ubiquinol, uric acid and enzymes are present (Thiele et al., 2006). With that mix of compounds naturally present in the skin, the target to be treated by CAP can withstand oxidative stress conditions comparably well. On the other hand, CAP can deliver chemically very active species, such as hydroxyl radicals, atomic oxygen, singlet oxygen, or ozone. For the latter compound, squalene oxidation in a model system has been described (Wisthaler and Weschler, 2010). The oxidation of phospholipids in liquid-suspended liposomes by CAP treatment was also described (Maheux et al., 2016; Yusupov et al., 2017). Accordingly, a substantial impact was expected.

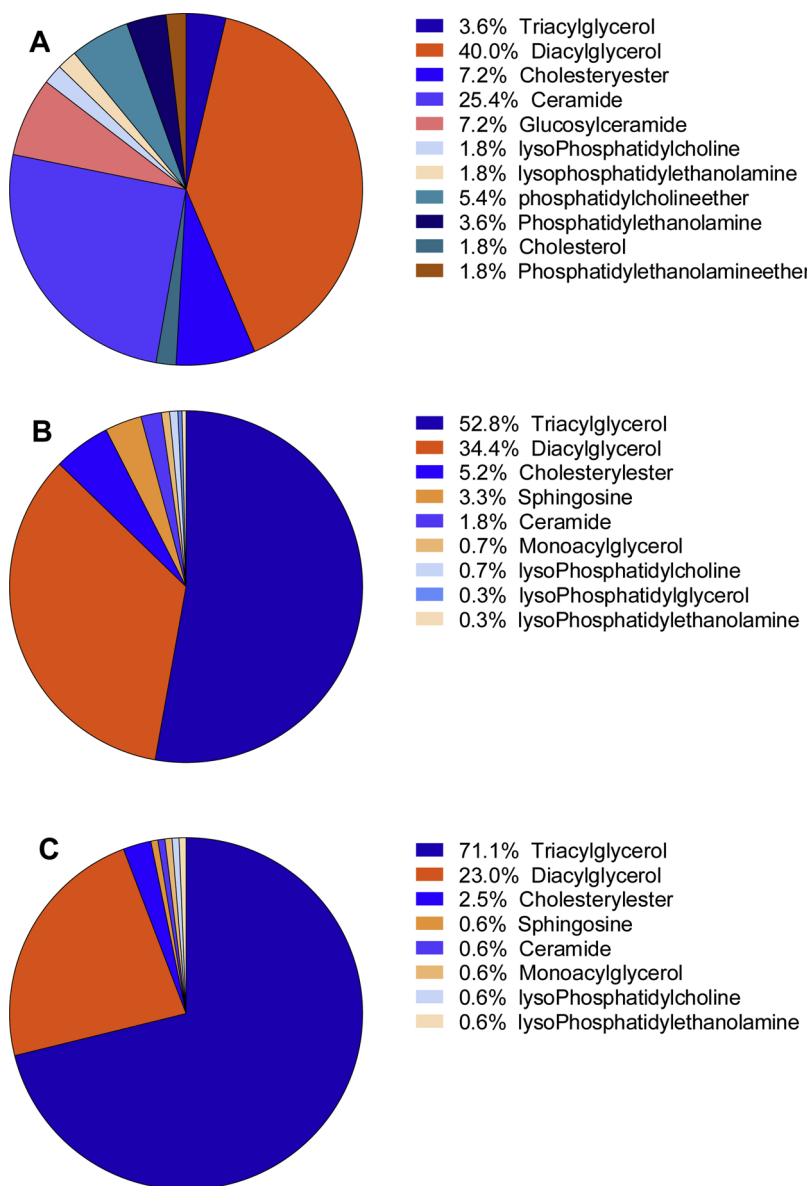


Fig. 6. Distribution of detected lipid classes and species thereof as identified by DI-MS² using LipidXplorer (A, combined before and after treatment) and LC/MS²/LipidSearch before (B) and after CAP (C) treatment. The most obvious difference between both approaches is the dominance of TGs in B/C compared to A that can be attributed to the sample workup procedure (see text).

Immediately after CAP treatment, analysis of the sampled lipids was performed using DI-MS² and RP-LC/MS². Using both approaches allowed us to compare the performance and handling of direct infusion and chromatographic separation regarding the identified lipid species, classes, and their distribution with a specific focus on oxidized lipids. Using DI-MS², most of the abundant *stratum corneum* and sebum lipids was observed. In the RP-LC/MS² approach, significant numbers of skin lipids were found with a lower diversity than those in DI-MS² experiments. Interestingly, triacylglycerols, which make up to 45–50 % of total sebaceous lipids (Pappas, 2009) showed contradicting proportions of the total lipids observed by both approaches. The cause may be the different extraction methods used for both approaches. Triacylglycerols are of neutral charge and are extracted best using hydrophobic solvents such as chloroform or ether (Ferraz et al., 2004). For RP-LC/MS², MTBE was used, which is a hydrophobic solvent and, according to our data, mostly suitable for triacylglycerol extraction. For DI-MS², a mixture of chloroform, isopropanol and methanol was used, as reported in several studies, to extract polar lipids such as glycerophospholipids (Ferraz et al., 2004). This is reflected in the data by the overall larger diversity

of lipid classes (neutral and polar lipids) measured with DI-MS². Additionally, solvent systems could contribute to ionization efficiency of the samples, since ESI response is a function of solvent composition and some solvents (e.g., isopropanol and methanol) are reported to increase sensitivity and result in a better spray stability (Kostianen and Kauppila, 2009). To keep both approaches comparable, solvents for DI-ESI/MS², and RP-LC/MS² were composed of methanol and isopropanol (see Material and Methods section).

In conclusion, RP-LC/MS² seems to be favorable when investigating skin-derived triacylglycerols. In contrast to triacylglycerols, ceramides, a class of epidermal surface lipids, were detected in a larger diversity and in most of the study participants only in DI-MS². After chromatographic separation, sphingosine, a sphingoid base, was more abundant than ceramide but still in a lesser amount and in a few participants ($n = 17$ in untreated samples, $n = 3$ in treated samples). Additionally, in negative mode measurements, hydroxy fatty acids could be identified and were reported to be ceramide precursors. Research performed by t'Kindt et al. focusing on skin ceramides also used RP-LC/MS² but detected a larger diversity of ceramide species (t'Kindt et al., 2012).

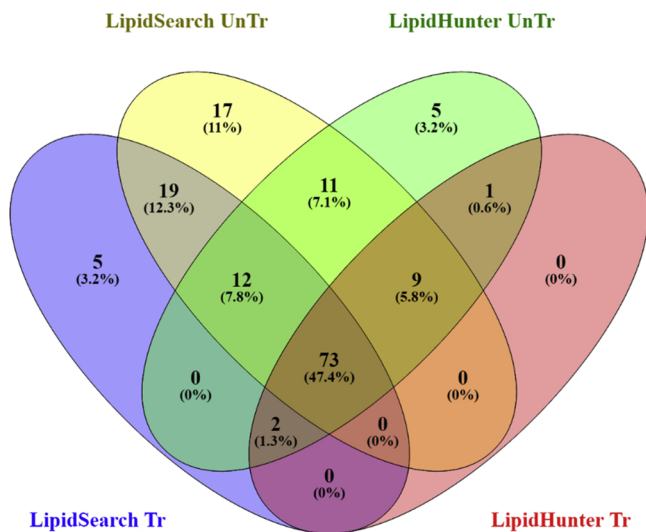


Fig. 7. Number of triacylglycerol subspecies identified with LipidSearch and LipidHunter in untreated (UnTr) and plasma-treated (Tr) skin lipid samples, see text. Figure created with Venny 2.1.0 web tool (Oliveros, 2007).

However, a minimally invasive tape-stripping method was used that collects larger portions of the epidermal surface lipids. Neither in our DI-MS² nor in LC/MS² experiments were phosphatidylcholines detected, although they are a major component of cell membranes (Van Meer et al., 2008). This clearly shows that the noninvasive approach used here emphasized the sebaceous gland lipids because the phosphatidylcholines are present in the viable layers of the skin mostly and, to a lesser extent, in the corneocytes of the *stratum corneum* (Plewig and Kligman, 2000). As expected, the abundance of lipid species was strongly modulated by interindividual variability. In conclusion, the overall picture of lipids and lipid classes detected suggests that using both MS acquisition techniques to study complex matrices improved the coverage of the lipid classes.

Using both MS-acquisition approaches also facilitate the testing of different Lipidomics software because most software is available for one approach and only in rare cases for both. LipidXplorer can be used exclusively for direct infusion analysis and identifies lipids down to the subspecies level (Herzog et al., 2013). Its molecular fragmentation query language (MFQL) allows users to build their own library to target specific lipid classes (Herzog et al., 2011). Regarding the CAP-derived oxidants, this allowed the search for lipid oxidation products with specifically designed mfql files. For LC/MS² analysis, LipidSearch (4.02) and LipidHunter (beta version) was used. The current LipidSearch versions did not allow the implementation of specialized libraries, limiting the identification capabilities for modified (oxidized) lipids potentially unique to plasma treatment. However, the inbuild oxGPL database provided a basic variety of lipid oxidation products. Although there were more triacylglycerol subspecies identified with LipidSearch, the identified subspecies from LipidHunter were largely identical.

For DI-MS², mono-oxidation was found for ceramides, triglycerides, and cholesteryl esters. In contrast, RP-LC/MS² detected oxidation in triglycerides only, primarily truncations of a fatty acid chain. When regarding the CAP derived reactive species portfolio, OH radicals, atomic oxygen, ozone, and singlet oxygen are most relevant suspects to initiate the oxidation. Along the classic lipid peroxidation pathway, a hydroxyl radical attack leads to a lipid radical (L^{\cdot}), and addition of molecular oxygen forms the corresponding hydroperoxyl radical (LOO^{\cdot}) and subsequently propagation or termination. The hydroperoxide may undergo Hock rearrangement, leading to the observed short chain aldehydic or dicarboxylic acid residues in the triglycerides and volatile compounds (not observed, see below). An alternate mechanism starts with singlet oxygen ${}^1\text{O}_2$ abstracting the allylic hydrogen, forming

L^{\cdot} (Sankhagowit et al., 2014). The impact of atomic O is rarely debated, as its formation is not trivial. Attacking of $\text{C}=\text{C}$ double bonds is fast and yield epoxides, aldehydes, or ketones via a short-lived 1,3 biradical (Havel, 1974). The mono-oxidation observed could correspond to both the epoxide (the major product according to the literature) and the oxo-derivatives requiring a 1,2-hydrogen migration (Gaffney et al., 1976). A substantial etching was described for olefins and polyolefins treated by atomic oxygen, with CO and CO_2 release from the treated material (Bès et al., 2018). Here, no loss of material was detected indicating that this process is not major. Overall, the number of observed oxidations was small compared to expectations, regardless of the approach used (DI-MS² or RP-LC/MS²) used. This is in contrast to the expected impact of the reactive oxygen species produced by the plasma treatment. Several possible reasons may be discussed: a) CAP-derived ROS do breakdown the lipids to volatile products, b) CAP-derived ROS are too weak or scavenged by the natural occurring antioxidants, c) the extraction of the oxidized lipids is ineffective, and d) the detection of the oxidized lipids is ineffective due to limitations of the software used. Regarding the first point, it can be stated that the weight of the sample-loaded cover slips has not been changed by the treatment (the weighing error of the balance was 0.001 mg). If volatile components occur, they occur in trace amounts. Additionally, the residual lipid with a shorter chain should remain as long as the reaction is not complete, but these were not detected. However, a solid-phase micro extraction gas chromatography approach will be performed in the future to further clarify this point and to estimate a potential balance between losses due to volatile compound formation and gain of mass due to oxygen addition to unsaturated lipid structures. Second, according to the composition of the human epidermis and unlike most other approaches investigating the biochemical impact of CAP, the model used here allows direct interaction of the reactive species with the target molecules without water as the modulator or amplifier. The gas-water interface is a significant barrier for many gaseous reactive species, and the lifetime in water is massively decreased; however, water itself can act as a massive source of hydroxyl radicals—e.g., by vacuum ultraviolet photolysis or electron impact. The resulting OH radicals are very effective and have been determined to be relevant (Banaschik et al., 2018). Despite the short lifetime, it has been suggested that OH radicals can “migrate” in aqueous liquids via a hydrogen shift (Verlackt et al., 2017). Thus, it might be assumed that water is one prerequisite for treatment effectiveness. This notion is emphasized by observations from Lackmann et al., showing that the protein RNase is inactivated in solution more rapidly than in dry conditions (Lackmann et al., 2015), indicating that skin lipids may have been affected to a lesser extent only. According to that, the long-term effects cannot be discussed in this study, since an analysis of the dry target at a later point will result in naturally air-oxidized lipid species. If the target to be treated would be in a liquid, short-lived as well as long-lived reactive species could interact with the lipids and might introduce more modifications to the target.

Additionally, natural antioxidants such as vitamin C and glutathione can be present in the lipid sample, stemming from the membrane (vitamin E) or cytosol (Pullar et al., 2017). Points 3 and 4 of the list are difficult to answer. Because MTBE was used as the extraction solvent for the RP-LC/MS² approach, the polar oxidized lipids may have only inefficiently been extracted. By contrast, the isopropanol/chloroform/methanol mix used in DI-MS² is sufficiently polar to dissolve phospholipids but did not improve the identification of oxidized species. In contrast to the proteomics field, where software tools have reached significant power in identifying even unknown amino acid sequences and hundreds of posttranslational modifications, this state has not been achieved in lipidomics so far. While good coverage for normal, unmodified lipids from complex samples can be achieved on the MS² level, limitations occur with respect to unexpected structures. Neither the self-designed mfql-file for LipidXplorer nor the offered oxGPLdatabase in LipidSearch nor the code of the LipidHunter covers all chemical modifications possible and may overlook the CAP-derived lipid

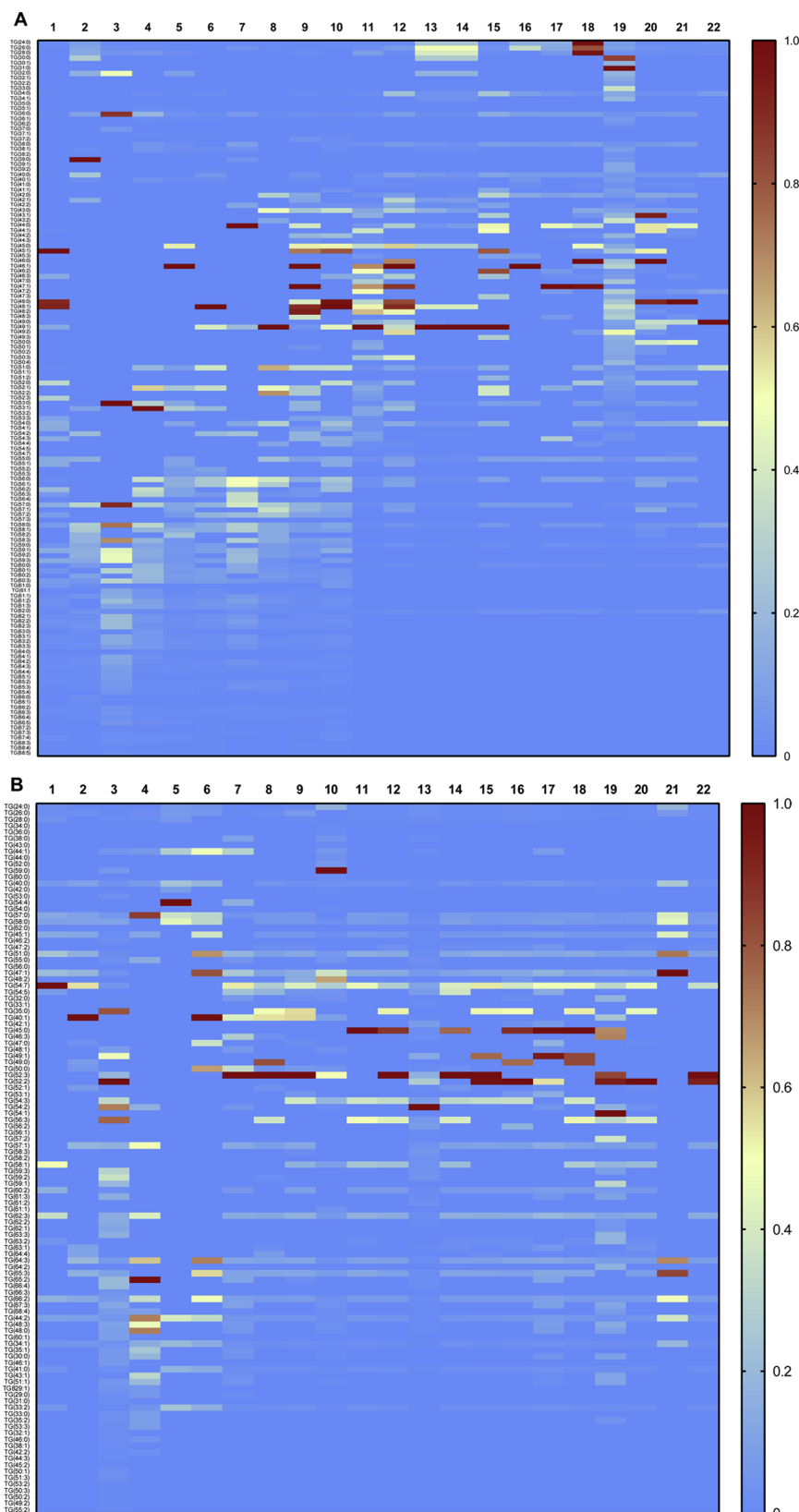


Fig. 8. Triacylglycerol subspecies identified with UHPLC/MS and LipidSearch before (A) and after (B) plasma treatment by sample, reflecting intraindividual variability. Saturated TGs dominate, but mono- and double unsaturated compounds are frequent. Treatment increases variance of abundance indicating differences in antioxidant presence in the sampled skin. Normalized data. Triacylglycerol subspecies identified with LipidHunter are shown in Fig. S1 in the supporting information.

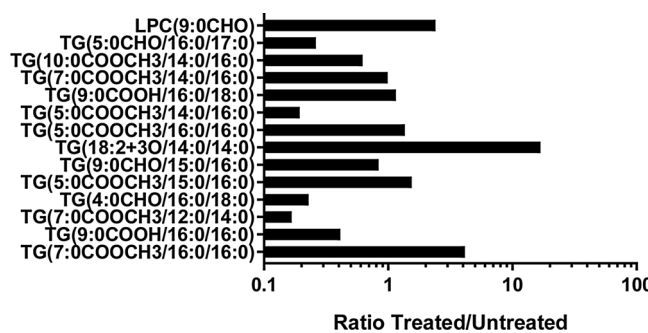


Fig. 9. Ratio between oxidized species in plasma-treated and untreated skin lipid samples, as identified by LipidSearch/oxGPL after RP18 UHPLC/electrospray MS.

oxidation products. However, now, it cannot easily be tested whether this assumption is correct because the other three points discussed must be addressed beforehand. Concerning the intended or performed applications of CAP in the medical field (e.g., promotion of wound healing) (Arndt et al., 2013), the observed results imply that accidental treatment of the intact skin with its sebum/epidermal lipid overlay yields little oxidation and limited (if any) functional consequences in the underlying epidermal cells.

5. Summary and conclusion

In this study, a standardized approach to treat skin lipids with cold atmospheric plasma in an *ex vivo* model was developed. Subsequent analysis with direct-infusion MS/MS (DI-MS²) and reversed-phase liquid chromatography-MS/MS (RP-LC/MS²) provided insight into skin lipid class diversity and lipid oxidation products derived from plasma treatment. Significant differences between the two approaches and subsequent software-based lipid species identifications were observed, indicating that, for complex mixtures, multiple approaches increase data comprehensiveness. Although expected to be different, skin lipids are oxidized to a minimal amount by the treatment. Possibly, the role of water as a modulator and supplier of reactive species is more important than so far recognized. However, the underestimation of lipid oxidation may be due to limitations in the extent of available databases for oxidative modifications or oxidation product type (volatile?), indicating the need for further research. Concerning the application of CAP in the medical field, the limited extent of oxidation suggests that accidental treatment of the intact skin with its sebum/epidermal lipid overlay yields limited (if any) functional consequences in the underlying tissue.

Acknowledgments

K.W. acknowledges funding from the German Federal Ministry of Education and Research (BMBF, grant number 03Z22DN12). M.F. acknowledges financial support from German Federal Ministry of Education and Research (BMBF) within the framework of the e:Med research and funding concept for SysMedOS project. Helpful comments and discussions with Dr. Sander Bekeschus are kindly acknowledged.

Appendix A. Supplementary data

Supplementary material related to this article can be found, in the online version, at doi:<https://doi.org/10.1016/j.chemphyslip.2019.104786>.

References

- Alakura, N., Akamatsu, H., Numata, S., Matsusue, M., Mashima, Y., Miyawaki, M., Yamada, S., Yagami, A., Nakata, S., Matsunaga, K., 2014. Fatty acid compositions of triglycerides and free fatty acids in sebum depend on amount of triglycerides, and do not differ in presence or absence of acne vulgaris. *J. Dermatol.* 41 (12), 1069–1076.
- Arndt, S., Unger, P., Wacker, E., Shimizu, T., Heinlin, J., Li, Y.F., Thomas, H.M., Morfill, G.E., Zimmermann, J.L., Bosserhoff, A.K., Karrer, S., 2013. Cold atmospheric plasma (CAP) changes gene expression of key molecules of the wound healing machinery and improves wound healing in vitro and in vivo. *PLoS One* 8 (11), e79325.
- Banaschik, R., Jablonowski, H., Bednarski, P.J., Kolb, J.F., 2018. Degradation and intermediates of diclofenac as instructive example for decomposition of recalcitrant pharmaceuticals by hydroxyl radicals generated with pulsed corona plasma in water. *J. Hazard. Mater.* 342, 651–660.
- Bekeschus, S., Schmidt, A., Weltmann, K.-D., von Woedtke, T., 2016. The plasma jet kINPen – a powerful tool for wound healing. *Clin. Plasma Med.* 4 (1), 19–28.
- Bekeschus, S., Freund, E., Wende, K., Gandhirajan, R., Schmidt, A., 2018. Hmox1 upregulation is a mutual marker in human tumor cells exposed to physical plasma-derived oxidants. *Antioxidants* 7 (11), 151.
- Bès, A., Koo, M., Phan, T.L., Lacoste, A., Pelletier, J., 2018. Oxygen plasma etching of hydrocarbon-like polymers: part I modeling. *Plasma Process. Polym.* 15 (8).
- Bruggeman, P.J., Kushner, M.J., Locke, B.R., Gardener, J.G.E., Graham, W.G., Graves, D.B., Hofman-Carlis, R.C.H.M., Maric, D., Reid, J.P., Ceriani, E., Rivas, D.F., Foster, J.E., Garrick, S.C., Gorbaney, Y., Hamaguchi, S., Iza, F., Jablonowski, H., Klimov, E., Kolb, J., Krcma, F., Lukes, P., Machala, Z., Marinov, I., Mariotti, D., Thagard, S.M., Minakata, D., Neyts, E.C., Pawlat, J., Petrovic, Z.L., Pflieger, R., Reuter, S., Schram, D.C., Schroter, S., Shiraiwa, M., Tarabova, B., Tsai, P.A., Verlet, J.R.R., von Woedtke, T., Wilson, K.R., Yasui, K., Zvereva, G., 2016. Plasma-liquid interactions: a review and roadmap. *Plasma Sources Sci. Technol.* 25 (5).
- Camera, E., Ludovici, M., Tortorella, S., Sinagra, J.-L., Capitanio, B., Goracci, L., Picardo, M., 2016. Use of lipidomics to investigate sebum dysfunction in juvenile acne. *J. Lipid Res.* 57 (6), 1051–1058.
- Choi, S., Attri, P., Lee, I., Oh, J., Yun, J.H., Park, J.H., Choi, E.H., Lee, W., 2017. Structural and functional analysis of lysozyme after treatment with dielectric barrier discharge plasma and atmospheric pressure plasma jet. *Sci. Rep.* 7 (1), 1027.
- Eggers, L.F., Schwudke, D., 2018. Shotgun lipidomics approach for clinical samples. *Methods Mol. Biol.* 1730, 163–174.
- Emmert, S., Brehmer, F., Hänsle, H., Helmke, A., Mertens, N., Ahmed, R., Simon, D., Wandke, D., Maus-Friedrichs, W., Däschlein, G., Schön, M.P., Viöl, W., 2013. Atmospheric pressure plasma in dermatology: ulcer treatment and much more. *Clin. Plasma Med.* 1 (1), 24–29.
- Ferraz, T.P.L., Fiúza, M.C., dos Santos, M.L.A., Pontes de Carvalho, L., Soares, N.M., 2004. Comparison of six methods for the extraction of lipids from serum in terms of effectiveness and protein preservation. *J. Biochem. Biophys. Methods* 58 (3), 187–193.
- Gaffney, J., Atkinson, R., Pitts Jr., J., 1976. Reaction of oxygen (3P) atoms with toluene and 1-methylcyclohexene. *J. Am. Chem. Soc.* 98 (7), 1828–1832.
- Golda, J., Held, J., Redeker, B., Konkowski, M., Beijer, P., Sobota, A., Kroesen, G., Braithwaite, N.S.J., Reuter, S., Turner, M.M., Gans, T., O'Connell, D., Schulz-von der Gathen, V., 2016. Concepts and characteristics of the 'COST reference microplasma jet'. *J. Phys. D Appl. Phys.* 49 (8).
- Gorbaney, Y., Stehling, N., O'Connell, D., Chechik, V., 2016. Reactions of nitroxide radicals in aqueous solutions exposed to non-thermal plasma: limitations of spin trapping of the plasma induced species. *Plasma Sources Sci. Technol.* 25 (5), 055017.
- Gorbaney, Y., Verlackt, C.C.W., Tinck, S., Tuenter, E., Foubert, K., Cos, P., Bogaerts, A., 2018. Combining experimental and modelling approaches to study the sources of reactive species induced in water by the COST RF plasma jet. *Phys. Chem. Chem. Phys.* 20 (4), 2797–2808.
- Havel, J.J., 1974. Atomic oxygen. I. Reactions of allenes with oxygen (3P) atoms. *J. Am. Chem. Soc.* 96 (2), 530–533.
- Herzog, R., Schwudke, D., Schuhmann, K., Sampaio, J.L., Bornstein, S.R., Schroeder, M., Shevchenko, A., 2011. A novel informatics concept for high-throughput shotgun lipidomics based on the molecular fragmentation query language. *Genome Biol.* 12 (1), R8.
- Herzog, R., Schwudke, D., Shevchenko, A., 2013. LipidXplorer: software for quantitative shotgun lipidomics compatible with multiple mass spectrometry platforms. *Curr. Protoc. Bioinformatics* 43 (12), 11–30.
- Iseni, S., Zhang, S., van Gessel, A.F.H., Hofmann, S., van Ham, B.J.T., Reuter, S., Weltmann, K.D., Bruggeman, P.J., 2014. Nitric oxide density distributions in the effluent of an RF argon APPJ: effect of gas flow rate and substrate. *New J. Phys.* 16 (12), 123011.
- Jablonowski, H., Sousa, J.S., Weltmann, K.-D., Wende, K., Reuter, S., 2018. Quantification of the ozone and singlet delta oxygen produced in gas and liquid phases by a non-thermal atmospheric plasma with relevance for medical treatment. *Sci. Rep.* 8 (1), 12195.
- Klinkhammer, C., Verlackt, C., Smilowicz, D., Kogelheide, F., Bogaerts, A., Metzler-Nolte, N., Stapelmann, K., Havenith, M., Lackmann, J.W., 2017. Elucidation of plasma-induced chemical modifications on glutathione and glutathione disulphide. *Sci. Rep.* 7 (1), 13828.
- Kostiainen, R., Kauppinen, T.J., 2009. Effect of eluent on the ionization process in liquid chromatography-mass spectrometry. *J. Chromatogr. A* 1216 (4), 685–699.
- Lackmann, J.W., Baldus, S., Steinborn, E., Edengeiser, E., Kogelheide, F., Langlotz, S., Schneider, S., Leichert, L.I.O., Benedikt, J., Awakowicz, P., Bandow, J.E., 2015. A dielectric barrier discharge terminally inactivates RNase A by oxidizing sulfur-containing amino acids and breaking structural disulfide bonds. *J. Phys. D Appl. Phys.* 48 (49).
- Lackmann, J.W., Wende, K., Verlackt, C., Golda, J., Volzke, J., Kogelheide, F., Held, J., Bekeschus, S., Bogaerts, A., Schulz-von der Gathen, V., Stapelmann, K., 2018. Chemical fingerprints of cold physical plasmas - an experimental and computational study using cysteine as tracer compound. *Sci. Rep.* 8 (1), 7736.
- Lademann, O., Richter, H., Kramer, A., Patzelt, A., Meinke, M.C., Graf, C., Gao, Q., Korotianskiy, E., Rühl, E., Weltmann, K.D., Lademann, J., Koch, S., 2011a.

- Stimulation of the penetration of particles into the skin by plasma tissue interaction. *Laser Phys. Lett.* 8 (10), 758–764.
- Lademann, O., Richter, H., Meinke, M.C., Patzelt, A., Kramer, A., Hinz, P., Weltmann, K.D., Hartmann, B., Koch, S., 2011b. Drug delivery through the skin barrier enhanced by treatment with tissue-tolerable plasma. *Exp. Dermatol.* 20 (6), 488–490.
- Lukes, P., Dolezalova, E., Sisrova, I., Clupek, M., 2014. Aqueous-phase chemistry and bactericidal effects from an air discharge plasma in contact with water: evidence for the formation of peroxy nitrite through a pseudo-second-order post-discharge reaction of H₂O₂ and HNO₂. *Plasma Sources Sci. Technol.* 23 (1), 015019.
- Maheux, S., Frache, G., Thomanen, J.S., Clement, F., Penny, C., Belmonte, T., Duday, D., 2016. Small unilamellar liposomes as a membrane model for cell inactivation by cold atmospheric plasma treatment. *J. Phys. D Appl. Phys.* 49 (34), 344001.
- Nakashima, Y., Ikawa, S., Tanji, A., Kitano, K., 2016. Ion-exchange chromatographic analysis of peroxy nitric acid. *J. Chromatogr. A* 1431, 89–93.
- Ni, Z., Angelidou, G., Hoffmann, R., Fedorova, M., 2017a. LPPtiger software for lipidome-specific prediction and identification of oxidized phospholipids from LC-MS datasets. *Sci. Rep.* 7 (1), 15138.
- Ni, Z., Angelidou, G., Lange, M., Hoffmann, R., Fedorova, M., 2017b. LipidHunter identifies phospholipids by high-throughput processing of LC-MS and shotgun lipidomics datasets. *Anal. Chem.* 89 (17), 8800–8807.
- Oliveros, J., 2007. VENNY. An Interactive Tool for Comparing Lists With Venn Diagrams. BioinfoGP, CNB-CSIC. .
- Pappas, A., 2009. Epidermal surface lipids. *Dermatoendocrinology* 1 (2), 72–76.
- Plewig, G., Kligman, A.M., 2000. In: Plewig, G., Kligman, A.M. (Eds.), *Epidermal Lipids: ACNE and ROSACEA*. Springer Berlin Heidelberg, Berlin, Heidelberg, pp. 50–55.
- Pullar, J.M., Carr, A.C., Vissers, M.C.M., 2017. The roles of vitamin C in skin health. *Nutrients* 9 (8), 866.
- Reuter, S., Tresp, H., Wende, K., Hammer, M.U., Winter, J., Masur, K., Schmidt-Bleker, A., Weltmann, K.D., 2012a. From RONS to ROS: tailoring plasma jet treatment of skin cells. *IEEE Trans. Plasma Sci.* 40 (11), 2986–2993.
- Reuter, S., Winter, J., Schmidt-Bleker, A., Tresp, H., Hammer, M.U., Weltmann, K.D., 2012b. Controlling the ambient air affected reactive species composition in the effluent of an argon plasma jet. *IEEE Trans. Plasma Sci.* 40 (11), 2788–2794.
- Rödder, K., Moritz, J., Miller, V., Weltmann, K.-D., Metelmann, H.-R., Gandhirajan, R., Bekeschus, S., 2019. Activation of murine immune cells upon co-culture with plasma-treated B16F10 melanoma cells. *Appl. Sci.* 9 (4), 660.
- Sankhagowit, S., Wu, S.H., Biswas, R., Riche, C.T., Povinelli, M.L., Malmstadt, N., 2014. The dynamics of giant unilamellar vesicle oxidation probed by morphological transitions. *Biochim. Biophys. Acta* 1838 (10), 2615–2624.
- Schmidt, A., Dietrich, S., Steuer, A., Weltmann, K.-D., von Woedtke, T., Masur, K., Wende, K., 2015. Non-thermal plasma activates human keratinocytes by stimulation of antioxidant and phase II pathways. *J. Biol. Chem.* 290 (11), 6731–6750.
- Schmidt, A., Bekeschus, S., Jarick, K., Hasse, S., von Woedtke, T., Wende, K., 2019. Cold physical plasma modulates p53 and mitogen-activated protein kinase signaling in keratinocytes. *Oxid. Med. Cell. Longev.* 2019, 7017363.
- Schmidt-Bleker, A., Reuter, S., Weltmann, K.-D., 2014. Non-dispersive path mapping approximation for the analysis of ambient species diffusion in laminar jets. *Phys. Fluids* 26 (8), 083603 (1994–present).
- Schmidt-Bleker, A., Reuter, S., Weltmann, K.-D., 2015a. Quantitative schlieren diagnostics for the determination of ambient species density, gas temperature and calorimetric power of cold atmospheric plasma jets. *J. Phys. D-Appl. Phys.* 48 (17).
- Schmidt-Bleker, A., Winter, J., Bösel, A., Reuter, S., Weltmann, K.-D., 2015b. On the plasma chemistry of a cold atmospheric argon plasma jet with shielding gas device. *Plasma Sources Sci. Technol.* 25 (1), 015005.
- Schneider, S., Lackmann, J.W., Narberhaus, F., Bandow, J.E., Denis, B., Benedikt, J., 2011. Separation of VUV/UV photons and reactive particles in the effluent of a He/O₂atmospheric pressure plasma jet. *J. Phys. D Appl. Phys.* 44 (29).
- t'Kindt, R., Jorge, L., Dumont, E., Couturon, P., David, F., Sandra, P., Sandra, K., 2012. Profiling and characterizing skin ceramides using reversed-phase liquid chromatography-quadrupole time-of-flight mass spectrometry. *Anal. Chem.* 84 (1), 403–411.
- Takai, E., Kitamura, T., Kuwabara, J., Ikawa, S., Yoshizawa, S., Shiraki, K., Kawasaki, H., Arakawa, R., Kitano, K., 2014. Chemical modification of amino acids by atmospheric-pressure cold plasma in aqueous solution. *J. Phys. D Appl. Phys.* 47 (28), 285403.
- Thiele, J., Barland, C.O., Ghadially, R., Elias, P.M., 2006. Permeability and Antioxidant Barriers in Aged Epidermis. *Skin Aging*. Springer, pp. 65–79.
- Tresp, H., Hammer, M.U., Weltmann, K.-D., Reuter, S., 2013. Effects of atmosphere composition and liquid type on plasma-generated reactive species in biologically relevant solutions. *Plasma Med.* 3 (1-2), 45–55.
- Ulrich, C., Kluschke, F., Patzelt, A., Vandersee, S., Czaika, V.A., Richter, H., Bob, A., Hutton, J., Painsi, C., Huge, R., Kramer, A., Assadian, O., Lademann, J., Lange-Asschenfeldt, B., 2015. Clinical use of cold atmospheric pressure argon plasma in chronic leg ulcers: a pilot study. *J. Wound Care* 24 (5) 196, 198–200, 202–193.
- Van Ham, B., Hoffmann, S., Brandenburg, R., Bruggeman, P., 2014. In situ absolute O_3 and NO densities in the effluent of a cold RF argon atmospheric pressure plasma jet obtained by molecular beam mass spectrometry. *J. Phys. D Appl. Phys.* 47 (22), 224013.
- Van Meer, G., Voelker, D.R., Feigenson, G.W., 2008. Membrane lipids: where they are and how they behave. *Nat. Rev. Mol. Cell Biol.* 9 (2), 112–124.
- Verlackt, C.C.W., Neyts, E.C., Bogaerts, A., 2017. Atomic scale behavior of oxygen-based radicals in water. *J. Phys. D-Appl. Phys.* 50 (11), 11LT01.
- von Woedtke, T., Metelmann, H.R., Weltmann, K.D., 2014. Clinical plasma medicine: state and perspectives of in vivo application of cold atmospheric plasma. *Contrib. Plasma Phys.* 54 (2), 104–117.
- Weltmann, K.D., von Woedtke, T., 2017. Plasma medicine-current state of research and medical application. *Plasma Phys. Control. Fusion* 59 (1), 014031.
- Weltmann, K.D., Kindel, E., Brandenburg, R., Meyer, C., Bussiahn, R., Wilke, C., Von Woedtke, T., 2009. Atmospheric pressure plasma jet for medical therapy: plasma parameters and risk estimation. *Contrib. Plasma Phys.* 49 (9), 631–640.
- Wende, K., Straßenburg, S., Haertel, B., Harms, M., Holtz, S., Barton, A., Masur, K., von Woedtke, T., Lindequist, U., 2014. Atmospheric pressure plasma jet treatment evokes transient oxidative stress in HaCaT keratinocytes and influences cell physiology. *Cell Biol. Int.* 38 (4), 412–425.
- Wende, K., Williams, P., Dalluge, J., Gaens, W.V., Aboubakr, H., Bischof, J., von Woedtke, T., Goyal, S.M., Weltmann, K.D., Bogaerts, A., Masur, K., Bruggeman, P.J., 2015. Identification of the biologically active liquid chemistry induced by a nonthermal atmospheric pressure plasma jet. *Biointerfaces* 10 (2), 029518.
- Winter, J., Wende, K., Masur, K., Iseni, S., Dunnbier, M., Hammer, M.U., Tresp, H., Weltmann, K.D., Reuter, S., 2013. Feed gas humidity: a vital parameter affecting a cold atmospheric-pressure plasma jet and plasma-treated human skin cells. *J. Phys. D-Appl. Phys.* 46 (29).
- Winter, J., Tresp, H., Hammer, M.U., Iseni, S., Kupsch, S., Schmidt-Bleker, A., Wende, K., Dunnbier, M., Masur, K., Weltmann, K.D., Reuter, S., 2014. Tracking plasma generated H₂O₂ from gas into liquid phase and revealing its dominant impact on human skin cells. *J. Phys. D-Appl. Phys.* 47 (28).
- Wisthaler, A., Weschler, C., 2010. Reactions of ozone with human skin lipids: sources of carbonyls, dicarbonyls, and hydroxycarbonyls in indoor air. *Proc. Natl. Acad. Sci.* 107 (15), 6568–6575.
- Yan, D., Xiao, H., Zhu, W., Nourmohammadi, N., Zhang, L.G., Bian, K., Keidar, M., 2017. The role of aquaporins in the anti-glioblastoma capacity of the cold plasma-stimulated medium. *J. Phys. D Appl. Phys.* 50 (5), 055401.
- Yusupov, M., Wende, K., Kupsch, S., Neyts, E.C., Reuter, S., Bogaerts, A., 2017. Effect of head group and lipid tail oxidation in the cell membrane revealed through integrated simulations and experiments. *Sci. Rep.* 7 (1), 5761.
- Zhang, S., van Gaens, W., van Gessel, B., Hofmann, S., van Veldhuizen, E., Bogaerts, A., Bruggeman, P., 2013. Spatially resolved ozone densities and gas temperatures in a time modulated RF driven atmospheric pressure plasma jet: an analysis of the production and destruction mechanisms. *J. Phys. D Appl. Phys.* 46 (20), 205202.
- Zhou, R., Zhou, R., Zhuang, J., Zong, Z., Zhang, X., Liu, D., Bazaka, K., Ostrikov, K., 2016. Interaction of atmospheric-pressure air microplasmas with amino acids as fundamental processes in aqueous solution. *PLoS One* 11 (5), e0155584.